Supplementary Material

Co-substitution of Zn^{2+}/Ge^{4+} pair within garnet phosphors activated by Er^{3+} for enhancing luminescence properties and optical thermometry

Yuanhao Chen, Xiaoshan Zhang, Yirong Liu, Haisheng Liu, Dechao Yu,* and Dawei Zhang

Engineering Research Center of Optical Instrument and System, The Ministry of Education, Shanghai Key Laboratory of Modern Optical System, University of Shanghai for Science and Technology, Shanghai 200093, China

*Corresponding authors: Dechao Yu, d.yu@usst.edu.cn

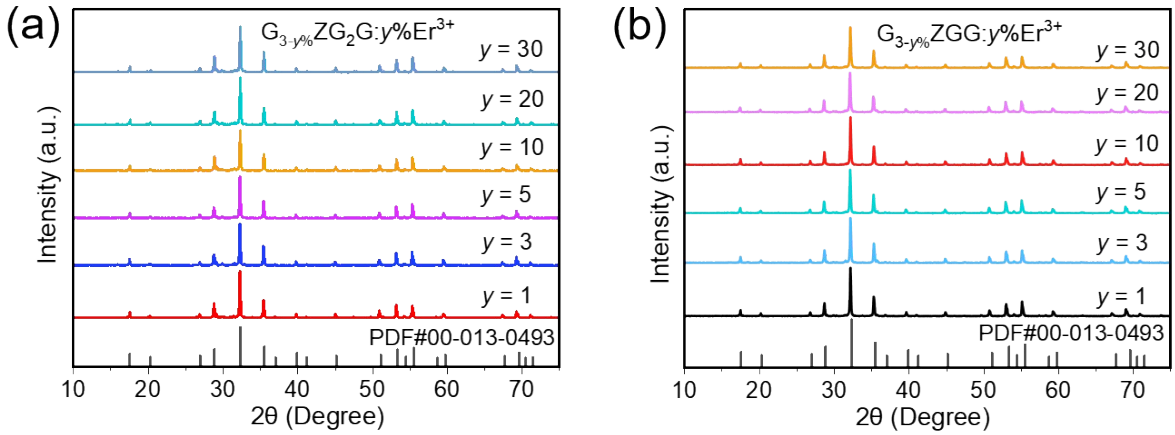

Fig. S1. XRD patterns of $G_{3-y\%}ZG_2G:y\%Er^{3+}$ (y = 1, 3, 5, 10, 20, 30) and $G_{3-y\%}ZGG:y\%Er^{3+}$ (y = 1, 3, 5, 10, 20, 30) phosphors obtained at room temperature, as well as that of the $Gd_3Ga_5O_{12}$ standard reference (PDF#00-013-0493).

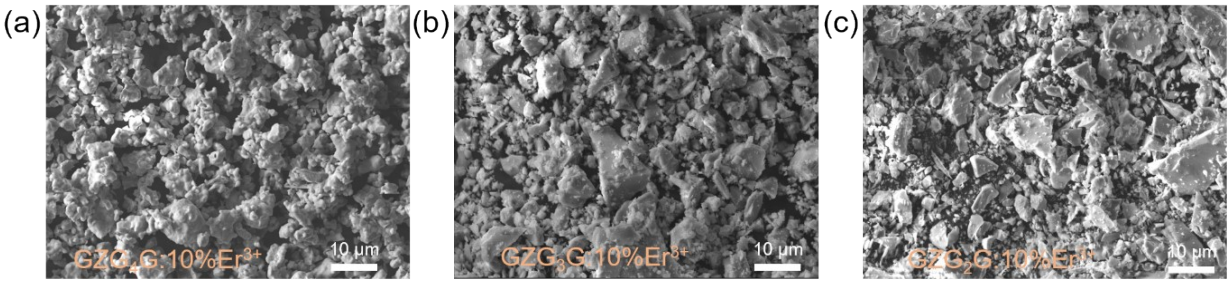

Fig. S2. SEM images of (a) $GZG_4G:10\%Er^{3+}$, (b) $GZG_3G:10\%Er^{3+}$ and (c) $GZG_2G:10\%Er^{3+}$ samples.

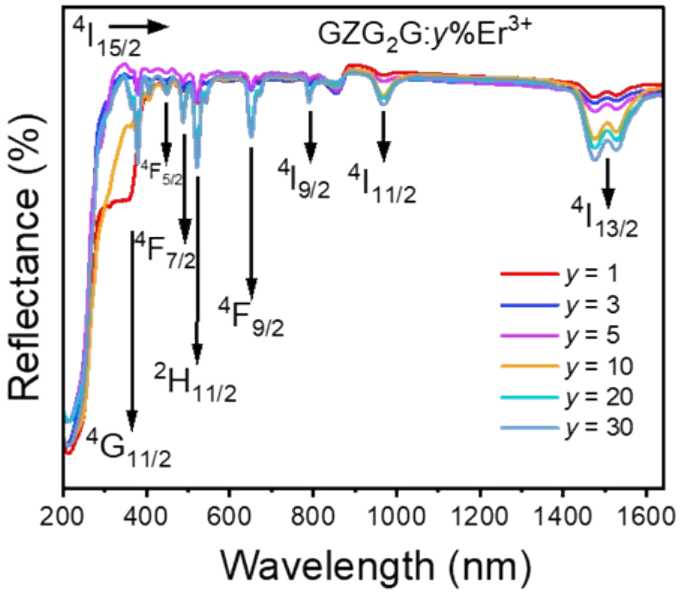

Fig. S3. Diffuse reflectance spectra of as-prepared $GZG_2G:y\%Er^{3+}$ (y = 1, 3, 5, 10, 20, 30) solid solution phosphors.

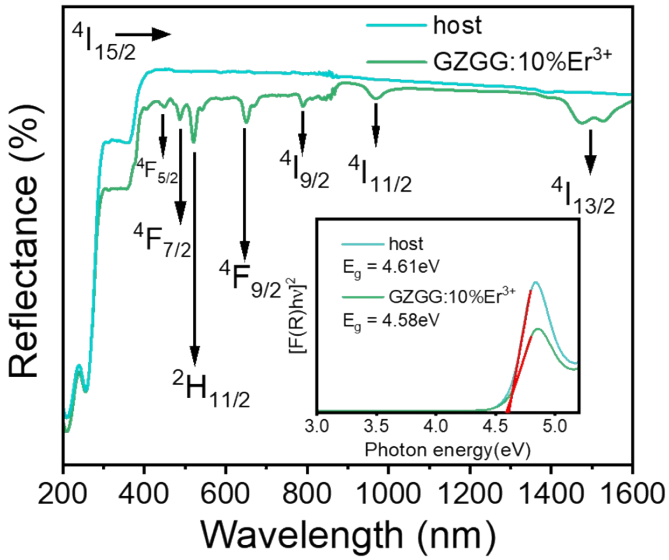

Fig. S4. Diffuse reflectance spectra and the band gap (E_g) of GZGG host and $GZGG:10\%Er^{3+}$ samples.

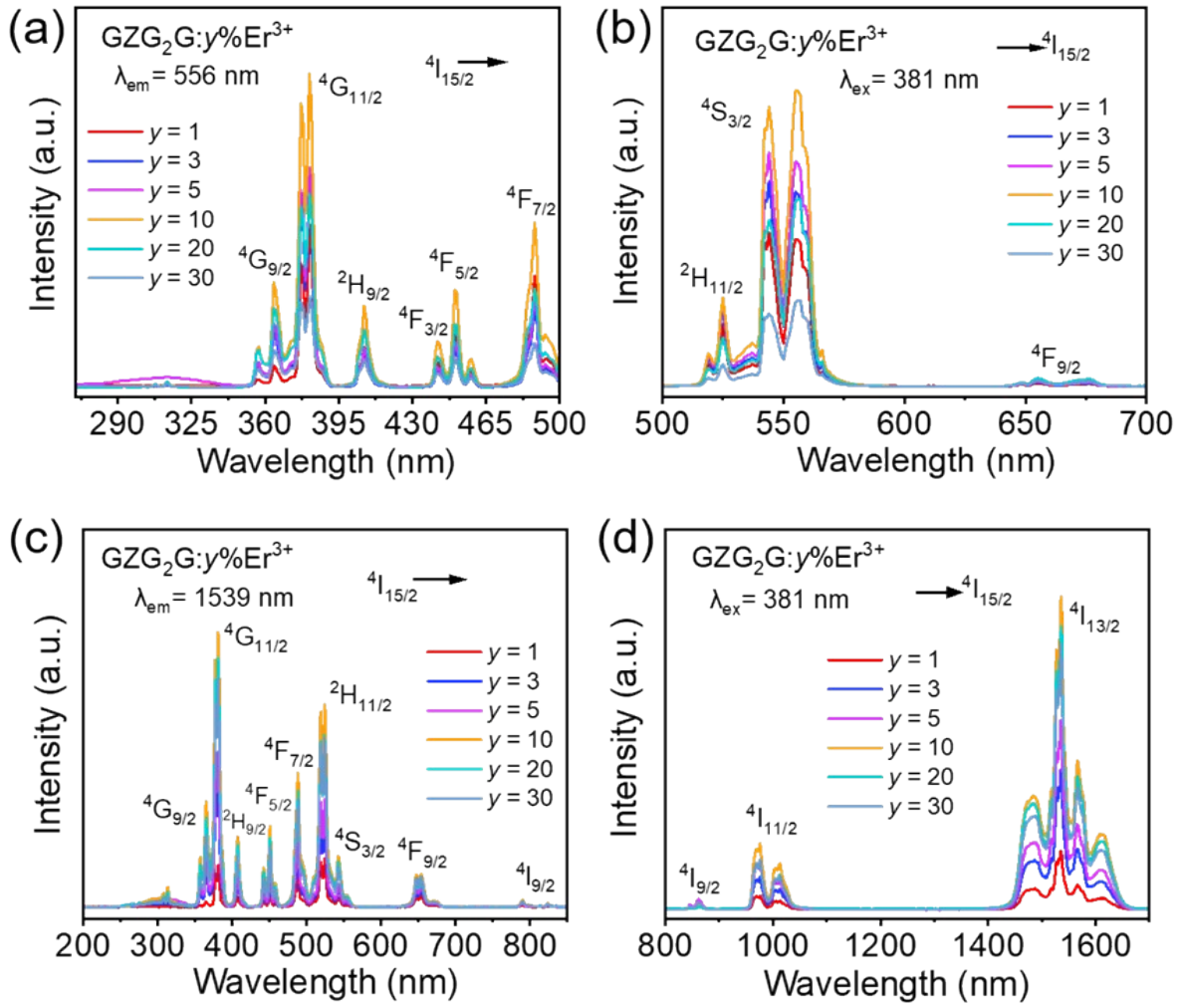

Fig. S5. (a) PLE spectra of $GZG_2G:y\%Er^{3+}$ (y = 1, 3, 5, 10, 20, 30) monitoring Er^{3+}: $^4S_{3/2} \rightarrow {}^4I_{15/2}$ transition at 556 nm and (c) that monitoring Er^{3+}: $^4I_{13/2} \rightarrow {}^4I_{15/2}$ transition at 1539 nm. (b) Visible PL and (d) NIR PL spectra of $GZG_2G:y\%Er^{3+}$ excited at 381 nm, respectively.

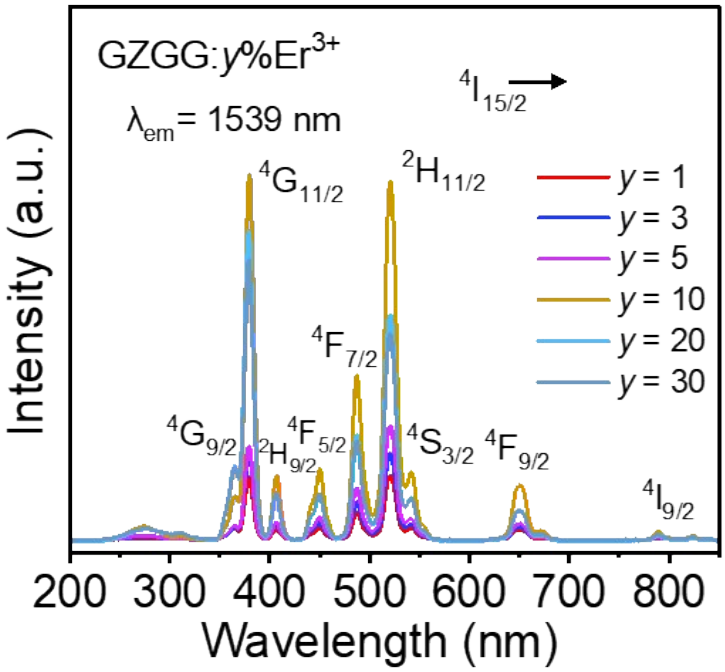

Fig. S6. PLE spectra of GZGG:*y*%Er^{3+} monitoring the $^4I_{13/2} \rightarrow {}^4I_{15/2}$ at ~ 1539 nm.

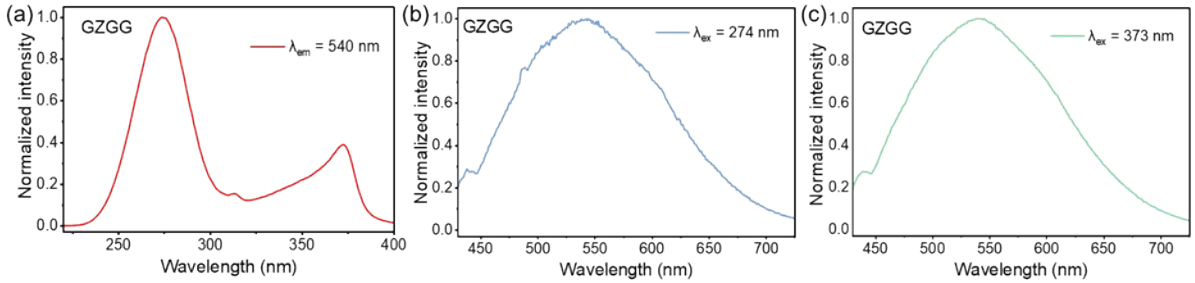

Fig. S7. Normalized visible PLE and PL spectra of the GZGG host matrix. The red curve is the PLE spectrum monitored at 540 nm (a), while the blue (b) and green (c) curves represent the PL spectra excited at 274 and 373 nm, respectively.

Table S1. Crystallographic data of $GZG_{5-2x}G$:10%Er^{3+} (x = 0.5, 1, 1.5, 2.0) with different chemical composite x values

Formula	x = 0.5	x = 1	x = 1.5	x = 2
Crystal system	Cubic			
Space group	Iad			
Lattice parameters				
a/b/c (Å)	12.47	12.47	12.67	12.74
α/β/γ (°)	90	90	90	90
2θ (°)	32.4	32.3	32.2	32.1
Cell volume ($Å^3$)	1939.10	1940.66	1945.44	1967.80
R_p	6.78	8.13	6.04	6.61
R_{wp}	8.99	11.81	8.10	7.69
χ^2	1.69	2.36	1.97	1.67

Table S2. Calculated decay time of Er^{3+} emission at ~ 556 nm ($^4S_{3/2} \rightarrow {}^4I_{15/2}$), as well as the fitting parameters and R-squared (R^2) values for the $GZG_{5-2x}G$:10%Er^{3+} (x = 0.5, 1, 1.5, 2) samples under pulsed light excitation of 381 nm. Fitting was performed using a bi-exponential decay model

$GZG_{5-2x}G$:	Green emission: $^4S_{3/2} \rightarrow {}^4I_{15/2}$ at ~556 nm							
	I_0(Background)	A_1(Amplitude of fast decay)	A_2(slow decay)	Decay time (μs)		α	β	R^2
x = 0.5	0.002	0.96	0.019	τ_1 ~ 118 τ_2 ~ 454.1	τ_{avr} ~124.6	0.982	0.018	0.9988
x = 1	0.001	0.753	0.219	τ_1 ~ 105.4 τ_2 ~ 176.5	τ_{avr} ~121.5	0.774	0.226	0.9995
x = 1.5	0.002	0.68	0.312	τ_1 ~ 71.0 τ_2 ~ 141.1	τ_{avr} ~ 93.0	0.685	0.315	0.9992
x = 2	0.001	0.912	0.073	τ_1 ~ 66.4 τ_2 ~ 194	τ_{avr} ~ 75.9	0.927	0.073	0.9993

Table S3. Optical temperature sensing performances of $GZG_3G:10\%Er^{3+}$ in comparison with other reported Er^{3+}-activated thermometric phosphors

Schemes	Materials	Temperature range (K)	Sr (% K^{-1})	Ref.
Er^{3+} $^2H_{11/2}$-$^4S_{3/2}$ TCLs	NSGM: Er^{3+}	298–488	0.87	1
	$MgMoO_4$: Er^{3+}	323–573	0.83	2
	Bi_3TeBO_9:$x$$Er^{3+}$	298–473	0.87	3
	LaOF:Er^{3+}	298–373	1.24	4
	$SrLaLiTeO_6$: Yb^{3+}, Er^{3+}	458–698	0.84	5
	$NaGdF_4$:Yb^{3+}, Er^{3+}	317–342	0.60	6
	Sr_3WO_6:Er^{3+}	303–513	0.56	7
	$GZG_3G:10\%Er^{3+}$	298–573	1.25	This work

References

1. Taleb, Z. E. A. A.; Saidi, K.; Dammak, M. The dual-model up/down-conversion green luminescence of $NaSrGd(MoO_4)_3$: Er^{3+} and its application for temperature sensing. RSC Adv. **2024**, 14 (12), 8366-8377.
2. Zheng, H.; Zhou, X.; Li, S.; Li, L.; Deng, Y.; Huang, J.; Yan, Y. Research on the luminescent and thermometric properties of $MgMoO_4$: Er^{3+}. Mater. Res. Bull. **2024**, 179, 112944.
3. Jiang, H.; Song, J.; Hu, Q.; Su, Y.; Wen, Q.; Liu, L.; Zhu, J. Up/down-conversion luminescence and optical thermometry of Er^{3+}-activated bismuth tellurium borate. J. Alloys Compd. **2024**, 1005, 176002.
4. Rakov, N.; Matias, F.; Porfirio, F.; Maciel, G. S. Optical thermometry exploring up-conversion and down-shifting of photons in LaOF:Er^{3+} ceramic powders. Ceram. Int. **2025**, 51, 55968-55979.
5. Gong, S.; Wu, R.; Han, Q.; Kong, D.; Wu, W. Lead-free perovskite $Rb_2Sn_{1-x}Te_xCl_6$with bright luminescence for optical thermometry and tunable white light emitting diodes. J. Mater. Chem. C **2022**, 10 (36), 13217-13224.
6. Liu, X. B.; Skripka, A.; Lai, Y. M.; Jiang, Y.; Liu, J. D.; Vetrone, F.; Liang, J. Y. Fast wide-field upconversion luminescence lifetime thermometry enabled by single-shot compressed ultrahigh-speed imaging. Nat. Commun. **2021**, 12, 6401.
7. Degda, N.; Patel, N.; Chaudhari, K.; Murthy, K. V. R.; Srinivas, M. Ratiometric thermometry using down-conversion luminescence and solid-state lighting application of Er^{3+} activated strontium tungstate phosphor. Phys. B: Condens. Mater. **2024**, 683, 415923